JACS
JOURNAL OF THE AMERICAN CHEMICAL SOCIETY

ARTICLE

pubs.acs.org/JACS

Excited State Kinetics in Crystalline Solids: Self-Quenching in Nanocrystals of 4,4′-Disubstituted Benzophenone Triplets Occurs by a Reductive Quenching Mechanism

Gregory Kuzmanich,[†] Sabrina Simoncelli,[‡] Matthew N. Gard,[†] Fabian Spänig,[§] Bryana L. Henderson,[†] Dirk M. Guldi,*[,§] and Miguel A. Garcia-Garibay*[,†]

[†]Department of Chemistry and Biochemistry, University of California, Los Angeles, California 90024-1569, United States

[‡]Departamento de Química Inorgánica, Analítica y Química Física, Facultad de Ciencias Exactas y Naturales, Universidad de Buenos Aires, Pabellón 2, Ciudad Universitaria, 1428 Buenos Aires, Argentina

[§]Department of Chemistry and Pharmacy & Interdisciplinary Center of Molecular Materials (ICMM), Friedrich-Alexander-Universität Erlangen-Nürnberg, Egerlandstrasse 3, 91054 Erlangen, Germany

Supporting Information

ABSTRACT: We report an efficient triplet state self-quenching mechanism in crystals of eight benzophenones, which included the parent structure (**1**), six 4,4′-disubstituted compounds with NH_2 (**2**), NMe_2 (**3**), OH (**4**), OMe (**5**), COOH (**6**), and COOMe (**7**), and benzophenone-3,3′,4,4′-tetracarboxylic dianhydride (**8**). Self-quenching effects were determined by measuring their triplet−triplet lifetimes and spectra using femtosecond and nanosecond transient absorption measurements with nanocrystalline suspensions. When possible, triplet lifetimes were confirmed by measuring the phosphorescence lifetimes and with the help of diffusion-limited quenching with iodide ions. We were surprised to discover that the triplet lifetimes of substituted benzophenones in crystals vary over 9 orders of magnitude from ca. 62 ps to 1 ms. In contrast to nanocrystalline suspensions, the lifetimes in solution only vary over 3 orders of magnitude (1−1000 μs). Analysis of the rate constants of quenching show that the more electron-rich benzophenones are the most efficiently deactivated such that there is an excellent correlation, $\rho = -2.85$, between the triplet quenching rate constants and the Hammet σ^+ values for the 4,4′ substituents. Several crystal structures indicate the existence of near-neighbor arrangements that deviate from the proposed ideal for "n-type" quenching, suggesting that charge transfer quenching is mediated by a relatively loose arrangement.

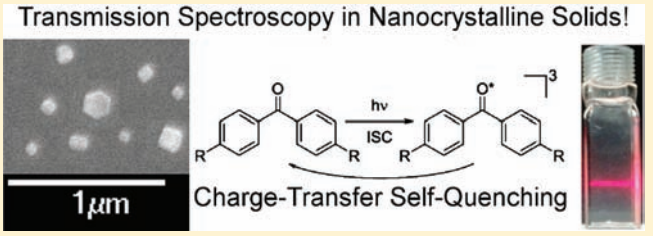

INTRODUCTION

The development of solid state photoresponsive devices requires advances in the fundamental knowledge of solid state photophysics[1] and photochemistry.[2] In particular, a deeper understanding of photophysical processes involving triplet states[3] has had a recent resurgence due to their importance in organic light-emitting diodes[4] and solar cells.[5] To study these processes, time-resolved transmission spectroscopy methods provide the most convenient and useful tool to analyze the generation, delocalization, and ultimate fate of the excited states. However, while studies in solution and in amorphous thin films are relatively simple, transient absorption measurements in crystalline solids are fraught with challenges that arise from their high optical densities, dichroism, birefringence, and light scattering.[6] Although some of these problems can be addressed with the use of diffuse-reflectance methods using dry powders, the need for high laser power combined with the efficient energy transfer[7] and delocalization of the excited state[8] often results in multiphotonic processes that could mask the intrinsic behavior of single excitations.[9]

We have recently shown that the use of nanocrystals with sizes smaller than the wavelength of light (ca. 200 nm) suspended in water minimizes many of the challenges associated with transient absorption methods. Crystalline molecular nanocrystals can be reproducibly obtained in water by the reprecipitation method pioneered by Kasai et al.[10] The method produces free-flowing, homogeneously dispersed organic nanoparticle suspensions with optical densities that can be tuned within a reasonable range by changing the nanocrystal loading. As crystal sizes decrease beyond the wavelength of individual photons and approach the limit of discrete supramolecular assembly samples, they can be excited in a nearly homogeneous manner, avoiding problems of penetration depth and diminishing their optical anisotropies. These characteristics permit nanocrystalline suspensions to be studied using transmission techniques analogous to those used in solution phase spectroscopy. It has been previously shown that

Received: May 28, 2011
Published: September 21, 2011

Table 1. Selected Photophysical Parameters of Benzophenones 1−8 in Acetonitrile Solutions, in Bulk Powder, and in Nanocrystalline Suspensions and the Average Particle Size in the Latter

		acetonitrile (ACN)			bulk	nanocrystalline				
	subst.	λ_{max} ($S_0 \rightarrow S_n$) nm	λ_{max} ($T_1 \rightarrow T_n$) nm	τ_{Abs} ($T_1 \rightarrow T_n$) μs	λ_{max} ($S_0 \rightarrow S_n$) nm	λ_{max} ($S_0 \rightarrow S_n$) nm	λ_{max} ($T_1 \rightarrow T_n$) nm	τ_{Abs} ($T_1 \rightarrow T_n$) μs	τ_{Em} ($T_1 \rightarrow S_0$) μs	avg size, nm
1	H	328 (n,π^*)	520	14	324 (n,π^*)	325 (n,π^*)	510	2.0	1.8	276
2	NH_2	330 (π,π^*)	560	10	348 (π,π^*)	345 (π,π^*)	595	6.2×10^{-5}	*d*	229
3	NMe_2	354 (π,π^*)	510[a]	11.4[a]	362 (π,π^*)	361 (π,π^*)	660	1.8×10^{-4}	*d*	328
4	OH	344 (π,π^*)	560	14	382 (π,π^*)	356 (π,π^*)	600	4.2×10^{-4}	*d*	281
5	OMe	339 (π,π^*)	545	3[c]	353 (π,π^*)	353 (π,π^*)	750	6.8×10^{-2}	0.068	236
6	COOH	314 (n,π^*)	540	20[b]	364 (n,π^*)	364 (n,π^*)	590	72	69	350
7	COOMe	312 (n,π^*)	545	170	293 (n,π^*)	296 (n,π^*)	595	97	84	236
8	$CO)_2O$	300 (n,π^*)	580	978	297 (n,π^*)	296 (n,π^*)	580	10^3	980	201

[a] Reference 24a. [b] Acquired in DMSO. [c] Reference 24b. [d] Emission not detected.

transmission UV−vis measurements of molecular nanocrystals suspended in water provides a simple means to assess particle sizes in terms of simple spectral shifts,[11] and we recently demonstrated that the use of organic nanocrystals of ca. 100−300 nm in size provides a simple method for measuring relative quantum yields and for quantitative analysis by transmission spectroscopy methods.[7,12]

We reported that the triplet lifetime of benzophenone determined by nanosecond transient absorption in a nanocrystalline suspension is characterized by a single exponential decay of 2 μs.[13] We noted that this lifetime is similar to that determined in solution[14] but very different from that obtained in dilute glasses at 77 K (8 ms)[15] or in bulk solids. The latter is best described as a complex multiexponential with components that range from tens of nanoseconds to milliseconds.[16] At the time of publication, the reason for the fast decay kinetics of nanocrystalline benzophenone was unknown. Subsequent experiments ruled out several possible causes, including multiphotonic interactions, dissolved oxygen, surfactants used to passivate the nanocrystal surfaces, and even the role of water with measurements carried out in deuterium oxide.[17] We found that anionic triplet quenchers such as iodide (I^-) deactivate the excited state at diffusion-limited rates, supporting a view of the nanocrystals as large supramolecular assemblies. Having ruled out the most obvious external quenching sources, we considered the possibility of self-quenching. Wolf et al.[18] and Schuster et al.[19] had shown in the early 1970s that the self-quenching of benzophenone triplets is quite efficient in solution, and two mechanisms were considered. The first mechanism, known as "n-type" quenching, involves electron donation from the ground state benzophenone aromatic ring into the electron-deficient oxygen lone pair orbital of the carbonyl group. The second mechanism, known as "π-type" quenching, involves donation of an electron from the half-filled π^* orbital of an excited benzophenone into the empty π^* orbital of the aromatic ring of a ground state molecule. Guttenplan and Favaro provided evidence supporting an n-type mechanism using electron-*donating* aromatics.[20−22] Schuster showed a correlation between the ionization potentials of electron-*withdrawing* substituted aromatic rings and quenching rate constants,[19] which is consistent with a mechanism of the π-type. Subsequently Wolf et al.[18] found a discontinuity at $\sigma^+ = 0$ with positive and negative slopes in the Hammet plot, indicating that both mechanisms can operate in solution.

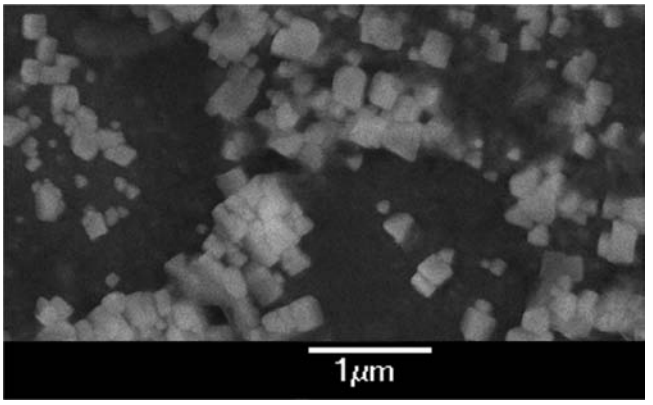

Figure 1. SEM images of 4,4′-diaminobenzophenone, **2**, showing faceted particles, most of them in the size range of ca. 150−300 nm.

Based on the above and given the close proximity between benzophenone molecules in their crystal, it seemed reasonable that intermolecular self-quenching could be responsible for the reduced triplet lifetime. To test this hypothesis, we chose a series of eight disubstituted benzophenones, **1**−**8**, that have varying electron-donating and -withdrawing substituents to systematically probe their effects on triplet lifetimes by transient absorption spectroscopy. The results indicate that triplet lifetimes range over 9 orders of magnitude from 10^{-12} to 10^{-3} s. There is a strong correlation between the excited state lifetimes, presumably reduced by self-quenching, and the electron-donating ability of the substituted benzophenones. A Hammet plot shows a good correlation between the σ^+ values of the substituents and the triplet lifetime of the respective benzophenones. From the slope, $\rho = -2.85$, we conclude that the triplet lifetimes of the substituted benzophenones in nanocrystalline suspensions are determined by the rate constant of self-quenching via a charge transfer mechanism that is consistent with the one expected by formation of an "n-type" exciplex.

RESULTS AND DISCUSSION

Synthesis and Purification of Benzophenone Derivatives. Compounds **1**−**6** and **8** are commercially available. Diester **7** was obtained by acid-catalyzed esterification of **6** with methanol.

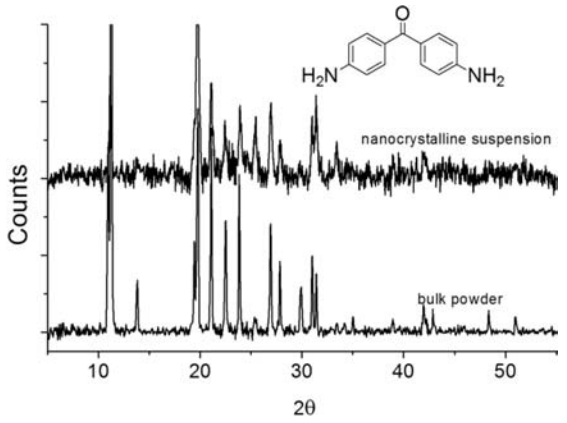

Figure 2. X-ray diffraction pattern of 4,4′-diaminobenzophenone, **2**, as the bulk powder and nanocrystalline suspension.

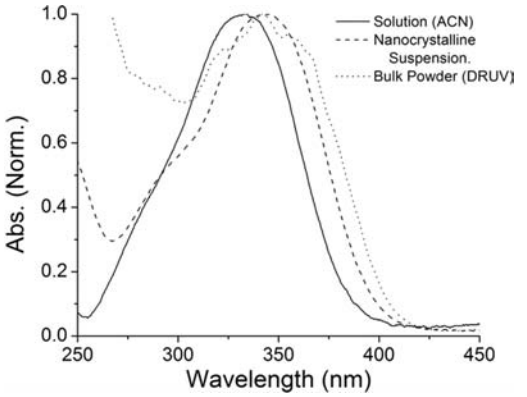

Figure 3. Transmittance UV−vis of 4, 4′-diaminobenzophenone, **2**. Only slight shifts in the λ_{max} of absorption are seen: λ_{ACN} = 330 nm, λ_{Susp} = 345 nm, λ_{DRUV} = 348 nm.

All compounds were purified immediately prior to use by Si-gel column chromatography using a mixture of hexane/ethyl ether (2:1 v/v) as the eluent, followed by recrystallization from hot ethanol.

Preparation and Characterization of Nanocrystalline Suspensions. The nanocrystalline suspensions were synthesized via the reprecipitation method[10] as described in the Experimental Section, which produces stable suspensions that can be easily transported in fluids such as water. The molecular nanoparticles were analyzed by dynamic light scattering (DLS) to determine their average size (Table 1) and distribution (Supporting Information, pp S4−S7). Although the average size of the nanocrystals varied between different compounds, the average particle size for a given compound was consistent between independent preparations.[23]

To confirm the average particle size determined by DLS, we also obtained scanning electron microscopy images (SEM) of the nanoparticles deposited on a Si wafer. Figure 1 illustrates a SEM image of 4,4′-diaminobenzophenone, **2**, nanocrystals showing discrete aggregates of a few faceted nanoparticles with sizes between 150 and 300 nm, consistent with values obtained in the DLS measurements. The SEM images for all other compounds agreed relatively well with the results obtained from the DLS measurements (Supporting Information, pp S4−S7). Using powder X-ray diffraction (PXRD) analysis of the bulk solids and filtered nanocrystalline samples, we were able to confirm that nanocrystals have the same crystal morphology (same polymorph) as the bulk samples. As illustrated in Figure 2 for 4,4′-diaminobenzophenone, **2**, the PXRD pattern of the nanocrystals matches very well with the bulk PXRD, with differences in their relative intensities suggesting the possibility of preferential orientations. Further confirmation that the bulk and nanocrystalline material are the same polymorph is that both melting points, as determined by differential scanning calorimetry, were identical (Supporting Information, pp S2, S3).

Ultraviolet (UV) Spectroscopy. Transmission UV spectroscopy is a fast, reliable method to differentiate between solution and nanocrystalline phases if the compound has significantly different absorption profiles in the respective states. The transmittance UV−vis spectra of the nanocrystals were generally similar to the UV−vis obtained by diffuse reflectance in bulk powders and consistent with those measured in solution (Supporting Information, pp S8, S9). In general, the ground state absorption for the nanocrystalline suspension showed a red shift from the corresponding UV spectrum in solution while the diffuse reflectance spectrum of the pure powders generally appeared broader. As an example, the UV−vis spectrum of 4,4′-diaminobenzophenone, **2**, shows a red shift of ca. 15 nm in bulk solid and nanocrystals compared with that in ACN (Figure 3). As shown in the figure, small differences were observed in the vibrational structure in the bulk and in nanocrystals. The lower energy (π,π^*)-rich transition in the hydroxy (**4**), methoxy (**5**), and amino substituted (**2** and **3**) samples is significantly stronger than in the (n,π^*)-rich transition of the parent compound (**1**) and the three structures with electron-withdrawing substituents (**6**, **7**, and **8**).

Nanosecond Laser Flash Photolysis in Solution. Transient absorption spectra were acquired for ketones **1**−**8** in ACN with OD ≈ 0.3 using λ_{ex} = 355 nm (<10 ns pulse width) from a Nd:YAG laser at concentrations that were low enough to avoid the self-quenching observed in solution.[18,19] All benzophenones produced a single transient with minimal vibrational resolution (S12−S18) with a λ_{max} between 460 and 560 nm that decayed monoexponentially with lifetimes that varied between 3 and 980 μs (Table 1). The results listed in Table 1 are in good agreement with known literature reports of disubstituted benzophenone lifetimes.[24] Although the transient absorption spectrum for the diester **7** has not been reported previously, a phosphorescence lifetime of 52.1 μs in acetonitrile was reported by Wang et al.[25] In our study, a relatively noisy triplet−triplet transient absorption with a λ_{max} at 545 nm in the same solvent revealed a lifetime of 140 ± 40 μs, which is consistent with our measured phosphorescence lifetime of 92 μs. Both the triplet−triplet absorption and the triplet emission in solution were very sensitive to oxygen, suggesting a possible reason for the differences between our lifetime measurements and the one reported previously.

A comparison of the values obtained with di-(*N*,*N*-dimethylamino)-benzophenone, **3** (Michler's ketone), and 4,4′-dimethoxybenzophenone, **4**, with the values reported for the analogous monosubstituted compounds indicates that the spectral features and lifetimes of the triplet state are not affected substantially by the second substituent.[24a,25] Based on this observation, we were able to support our assignments of the triplet absorption spectra and kinetics from 4,4′-diaminobenzophenone, **2**, and 4,4′-dihydroxybenzophenone, **4**. While triplet 4-aminobenzophenone has a lifetime of 11 μs and a λ_{max} at 560 nm in acetonitrile,[26] triplet 4,4′-diaminobenzophenone, **2**, has a lifetime of 10 μs and a λ_{max}

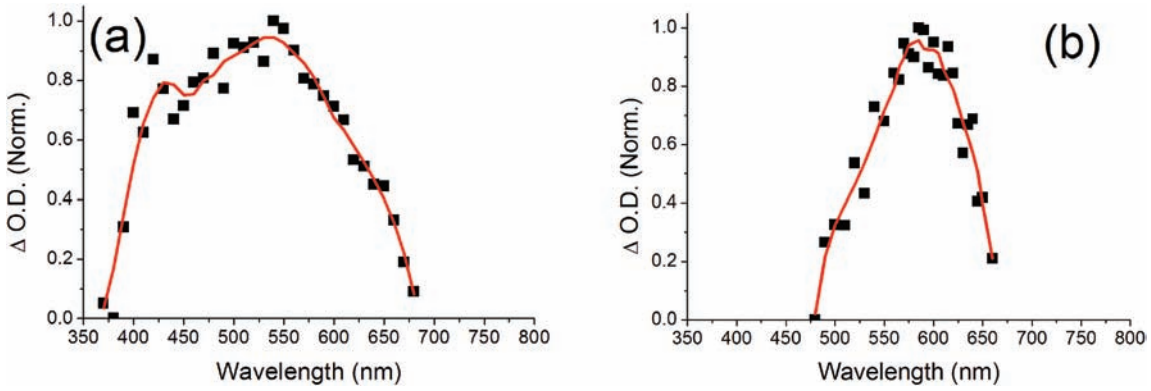

Figure 4. Nanosecond transient absorption spectrum (10 ns pulse, λ_{ex} = 355 nm) of diacid **6** (a) in DMSO and (b) as a nanocrystalline suspension.

at 560 nm in the same solvent. Similarly, while triplet 4-hydroxybenzophenone has a lifetime of 8 μs and a λ_{max} at 570 nm in acetonitrile,[27] we found that 4,4′-dihydroxybenzophenone, **4**, has a lifetime of 14 μs and a λ_{max} at 560 nm.

The nanosecond flash photolysis of diacid **6** and anhydride **8** have not been previously described. Pulsed excitation of diacid **6** in argon-saturated DMSO[28] revealed one band with a λ_{max} at 540 nm that spans from ca. 360 to 680 nm (Figure 4a) and uniformly decays with a monoexponential lifetime of 20 μs. As expected for a transient absorption corresponding to a triplet excited state, the band disappears when the solution is saturated with oxygen. We assign this band to the T_1 state of diacid **6**. Similarly, excitation of anhydride **8** in acetonitrile produces a band spanning from ca. 480 to 670 nm with a λ_{max} = 580 nm (Figure 5a) that is narrower than that of diacid **6**. The entire band decays monoexponentially with a lifetime of 978 μs (Table 1) and the corresponding carrier is also sensitive to molecular oxygen, in support of an assignment to the T_1 state of anhydride **8**.

Nanosecond Laser Flash Photolysis of Nanocrystalline Suspensions. Aqueous nanocrystalline suspensions with low particle loading prepared via the reprecipitation method display limited light scattering in the wavelength range of 350−800 nm and are suitable for transmission spectroscopy. The apparent absorbance used for these studies at λ_{ex} = 355 nm was 0.3. The spectra were acquired for both oxygenated (air and O_2) and deoxygenated (Ar) suspensions. As with solution samples, benzophenones **1** and **5**−**8** produced transients observed in the nanocrystalline suspension between 350 and 750 nm, which decayed monoexponentially with lifetimes that range between ca. 68 ns and 1 ms, as listed in Table 1. Nanocrystalline suspensions of **2**−**4** did not produce any transient signals with lifetimes >10 ns.

As a representative example, the transient absorption spectra of a nanocrystalline suspension of diacid **6** showed a relatively narrow absorption band between 475 and 650 nm with a λ_{max} at 590 nm (Figure 4b). This band decays uniformly with a lifetime of 80 μs and is insensitive to oxygen, as previously reported for nanocrystalline benzophenone.[17] This transient is slightly red-shifted and narrowed when compared with the spectrum observed in DMSO. In contrast, the transient spectrum obtained from an aqueous suspension of anhydride **8** is somewhat broadened and red-shifted compared with that obtained in acetonitrile (Figure 5b). The solid state spectrum has a λ_{max} at 580 and a shoulder at 650 nm. This band decays uniformly with a lifetime of 1 ms and was also unaffected by the presence of oxygen. Nanocrystalline suspensions of benzophenone **1**, the dimethoxy derivative **5**, and diester **7** produced analogous transient absorption spectra as **6** and **8** (Supporting Information, pp S12−S18). The transients in **1**, **5**, and **7** also decayed homogeneously and monoexponentially (Table 1). None of the transients were quenched by oxygen. In most cases, the observed solid state transients had a λ_{max} shifted by 30−40 nm relative to solution. We suspect that differences in the transient absorption spectra in solution and in nanocrystals may reflect variations in the electronic configuration of the triplet excited state, which is known to vary from pure n,π^* and pure π,π^* to mixed states and to be very sensitive to the nature of the environment. In fact, it is well documented that the T_1−T_n spectra of triplet ketones display shifts as large as 150 nm in different solvents. Restricted excited state relaxation in the rigid environment of the solid state may also contribute to differences between the spectra observed in solution and in nanocrystals. For compounds **2**−**4**, there were no observable transients within the time resolution (ca. 10 ns) of the nanosecond setup. However, the addition of ACN dissolved the nanocrystals and restored the transient signals that were analogous to those observed in the pure organic solvent.

Interfacial Quenching. While interfacial nanocrystal−solution quenching of the triplet excited states by molecular oxygen is inefficient due to both the low concentration of oxygen in water and the low affinity of oxygen for the organic crystalline surface, we recently showed that anionic quenchers known to act by an electron transfer mechanism[29] can be quite effective at the nanocrystal−water interface.[17] The triplet excited state of benzophenone is quenched by iodide with a rate constant coefficient that is analogous to that measured in solution, $k_q(I^-)$ = 7.4 × 10^9 M^{-1} s^{-1}. Given that the transients formed upon excitation of **1** and **5**−**8** were unaffected by oxygen, we decided to investigate the effect of added I^- to gain additional support of our excited state assignments. In fact, addition of aqueous NaI to nanocrystalline suspensions of **5**−**8** lead to complete quenching of the transient, supporting their assignments as excited states. Stern−Volmer experiments revealed that the effect of quencher concentration on the lifetimes of benzophenones **6**−**8** is linear, as expected for a purely dynamic quenching mechanism (Figure 6 and Supporting Information, pp S19, S20). The rate constants of quenching obtained from the slope of the Stern−Vomer plots are $k_q(I^-)$ = 2.4 × 10^8 M^{-1} s^{-1} for diacid **6**, $k_q(I^-)$ = 1.4 × 10^5 M^{-1} s^{-1} for diester **7**, and $k_q(I^-)$ = 1.1 × 10^6 M^{-1} s^{-1} for anhydride **8**. As expected from its short lifetime of only 68 ns, quenching of the dimethoxy **5** by I^- was difficult to quantify but easily observed in a qualitative manner.

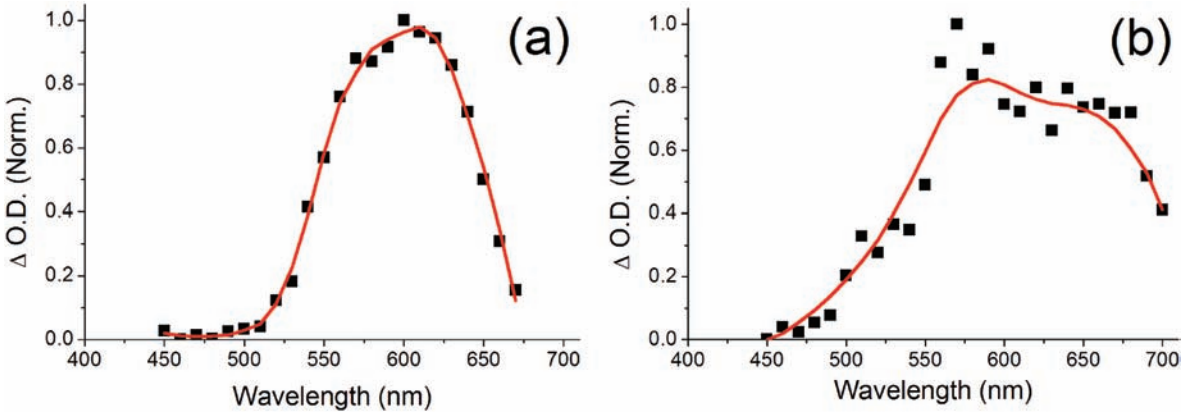

Figure 5. Nanosecond transient absorption spectrum (10 ns pulse, λ_{ex} = 355 nm) of anhydride **8** (a) in acetonitrile and (b) as a nanocrystalline suspension.

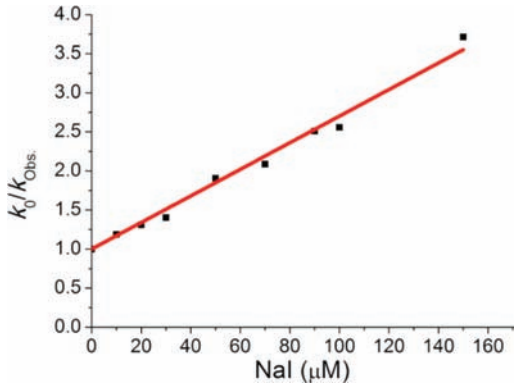

Figure 6. Stern−Volmer plot for the quenching of diacid **6** with NaI as a nanocrystalline suspension. The rate constant of quenching in this case is $k_q(I^-) = 1.4 \times 10^5\ M^{-1}\ s^{-1}$. The values of k_0 and k_{Obs} correspond to the rate constants in the absence of quencher and in the presence of added quencher, respectively.

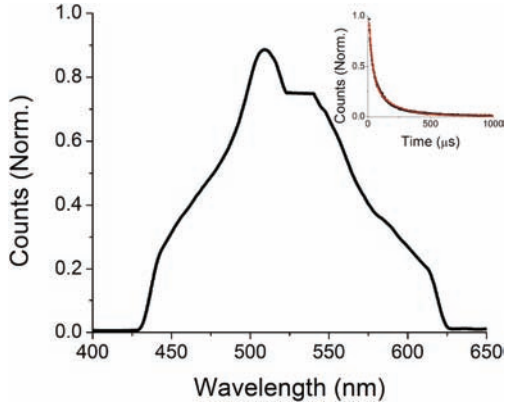

Figure 7. Phosphorescence spectrum of diacid **6** as a nanocrystalline suspension. Insert: Phosphorescence decay fitted to a lifetime of τ_{Em} = 69 μs, similar to that determined by flash photolysis (τ_{Abs} = 72 μs).

Phosphorescence Lifetimes. To confirm that the transients observed from the nanocrystalline suspensions correspond to the benzophenone T_1 states, their phosphorescence spectra and lifetimes were investigated at ambient temperature. As expected, no emission was observed from nanocrystalline samples of ketones **2**−**4**, which have very short lifetimes. However, reasonable signals were obtained for **1** and **5**−**8**. As an example, Figure 7 shows the phosphorescence spectrum from a nanocrystalline suspension of diacid **6** with a phosphorescence lifetime τ_{Em} = 69 μs, which is consistent with the lifetime of the transient absorption detected by flash photolysis with a value of τ_{Abs} = 72 μs. This excellent match strongly supports the assignment of the latter absorption signal as arising from the triplet excited state (T_1−T_n) rather than a ground state intermediate. Similar results were obtained for benzophenone (**1**), 4,4′-dimethoxybenzophenone (**5**), dimethyl ester (**7**), and dianhydride (**8**), which were found to have emission lifetimes of 1.8, 0.068, 84, and 980 μs, respectively (Supporting Information, pp S20, S21).

Femtosecond Transient Absorption. Given that the nanocrystalline suspensions of 4,4′-diaminobenzophenone (**2**), 4,4′-bis(dimethylamino)benzophenone (**3**), and 4,4′-dihydroxybenzophenone (**4**) did not show any observable transients after the 10 ns excitation pulse, we explored their transient absorption on a faster time scale. Because the results obtained with the amino-substituted compounds **2** and **3** in solution are relatively complex, we start by first describing our observations with 4,4′-dihydroxybenzophenone (**4**), which are relatively simpler and easier to interpret.

Excitation of 4,4′-dihydroxybenzophenone (**4**) as a nanocrystalline suspension using a 150 fs pulse at λ_{ex} = 258 nm resulted in a very broad transient that spans from ca. 440 to 730 nm, with λ_{max} at 460, 485, 535, 595, and 710 nm (Supporting Information, Figure S47). The decay of this transient could be fit to two overlapping components with lifetimes of 15 and 422 ps ($R^2 > 0.98$). The fast component primarily decreased the intensity of the absorption features at the two ends of the spectrum and the remaining longer-lived transient decayed uniformly with the 422 ps lifetime. The spectrum of 4,4′-dihydroxybenzophenone (**4**) in acetonitrile was also very broad, with a maximum near 550 nm and two shoulders at 480 and 600 nm (Supporting Information, Figure S46). Although relatively featureless, these results are in reasonable agreement with those reported by Bhasikuttan et al., who described the transient absorption of monosubstituted 4-hydroxybenzophenone using 35 ps pulses and assigned it to the triplet excited state.[27] It was shown that the spectra obtained in nonpolar aprotic benzene are relatively narrow, from ca. 460−600 nm, while those obtained in hydrogen bonding solvents such as methanol were broad and featureless, stretching from ca. 540 nm to more than 800 nm. Inspection of the single crystal

X-ray structure of 4,4′-dihydroxybenzophenone (**4**) shows that the benzophenone carbonyls are hydrogen bonded to the phenol hydrogen of an adjacent molecule in the lattice, which may help explain the much broader nature of the nanocrystal spectrum.[30] The shape and general location of triplet 4-hydroxybenzophenone match well with the spectra observed at long delays (>100 ps) for the nanocrystalline suspension of 4,4′-dihydroxybenzophenone, **4**. We propose that the initial transient corresponds to the singlet excited state, which undergoes intersystem crossing with a rate constant of $k_{ISC} = 6.5 \times 10^{10}\ s^{-1}$ to give the triplet state that has a lifetime of 422 ps. These assignments are in agreement with the intersystem crossing rate greater than $1.25 \times 10^{11}\ s^{-1}$ estimated for 4-hydroxybenzophenone by Ohtani et al.[31] Furthermore, the transient observed at long delay times (>100 ps) is qualitatively similar to the triplet observed in the nanosecond experiments in solution (Supporting Information, Figure S46).

Since it has been previously shown that the excited state dynamics of amino-substituted benzophenones are strongly solvent dependent,[32−34] it was not surprising that femtosecond excitation of 4,4′-bis(dimethylamino)benzophenone (**3**) produced different transients in acetonitrile and as a nanocrystal suspension. Excitation with 150 fs pulses at $\lambda_{ex} = 258$ nm in polar acetonitrile produced results in agreement with those reported by Mondel et al.,[32] which include up to four excited states within a spectral window from 450 to 1000 nm. It had been suggested that initial excitation leads into a local S_1 excited state (LE) characterized by a $\lambda_{max} = 650$ nm and a lifetime $\tau_1 = 0.45$ ps. In polar solvents, the LE state transforms into a new transient assigned as a singlet intramolecular charge transfer species, ICT, with a $\lambda_{max} = 950$ nm and a lifetime $\tau_{ICT} = 1.6$ ps. It was proposed that the ICT undergoes a conformational change to form a twisted charge transfer species, TICT, with a $\lambda_{max} = 700$ nm and a lifetime $\tau_{TICT} = 600$ ps (Supporting Information, Figure S43). Notably, Singh et al. had previously shown that excitation of **3** in nonpolar cyclohexane and benzene did not produce the charge transfer species.[33] Excitation at 310 nm using 500 fs pulses in cyclohexane led to the formation of the singlet state with a maximum at ca. 490 nm. Intersystem crossing in the nonpolar solvent occurs within 6.7 ps to form the triplet state with a λ_{max} at 510 nm. It was also suggested that high concentration of **3** lead to formation of aggregates, which were detected by a large red shift with a $\lambda_{max} \approx 700$ nm.

As expected for a medium with low polarity, excitation of nanocrystalline 4,4′-bis(dimethylamino)benzophenone (**3**) did not produce transients similar to the charge transfer states observed in acetonitrile. In agreement with the results from the suggested aggregates in concentrated benzene, excitation of nanocrystalline **3** gave rise to a broad transient that spans our entire observation window from 425 to 750 nm (Supporting Information, Figure S44). The absorption on the blue edge of this transient decays monoexponentially within 25 ps and a band centered at ca. 690 nm remains with a vibrational structure that has maxima at ca. 550, 610, and 680 nm. The latter transient decays monoexponentially with a lifetime of 180 ps, and no other transients were observed for up to 3 ns. The shape and location of the transient centered at 660 nm for 4,4′-bis(dimethylamino)-benzophenone (**3**) is very different from those obtained from the charge transfer states formed in polar solvents. However, there is a reasonably good agreement between the nanocrystal spectra and the spectra acquired upon excitation of the aggregates in benzene reported by Singh, which were also assigned to the triplet state.

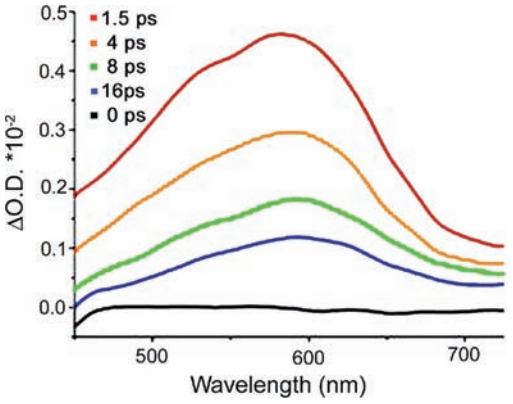

Figure 8. Femtosecond transient absorption spectroscopy of diaminobenzophenone (**2**; 150 fs pulse, $\lambda_{max} = 258$ nm) as a nanocrystalline suspension. ISC occurs within 5 ps to give the triplet, $\lambda_{max} = 595$ nm, which decays within 62 ps.

Finally, the excitation of 4,4′-diaminobenzophenone (**2**) in acetonitrile produced a similar charge-transfer species as the one detected from 4,4′-bis(dimethylamino)benzophenone (**3**), which will not be discussed in detail at this time. As shown in Figure 8, a transient spanning from 470 to 620 nm with $\lambda_{max} = 585$ nm forms upon excitation of a nanocrystalline suspension of **2**. Within 5 ps, there is a shift in the λ_{max} from 585 to 595 nm. The new band decays monoexponentially with a lifetime of 62 ps ($R^2 > 0.99$), and no other transients were observed up to 3 ns. As in the case of ketone **3**, none of the bands tentatively assigned to the charge transfer states in solution were observed in the nanocrystals at any time delay. Because the decay of the band at 585 nm occurs on time scales similar to that for ISC of benzophenones (5−10 ps) and given the similarity between the band centered at 595 nm and the triplet state observed on the nanosecond time scales in solution, we tentatively assign the two bands as arising from the singlet and triplet excited states, respectively.

Although the excitation of the amino-substituted benzophenones **2** and **3** leads to the formation of ICT and TICT structures in solution, there appears to be no formation of such transients upon excitation of the nanocrystals. Computational modeling of 4,4′-bis(dimethylamino)benzophenone (**3**) by Pal et al.[34] predicts that as the medium becomes less polar the excited state energy order is inverted. In acetonitrile, the local excitation (LE) is 85.8 kcal/mol above the ground state and the final twisted intramolecular charge transfer state (TICT) is 80.5 kcal/mol above the ground state. We postulate that the lack of observed charge transfer excited states in nanocrystals is due to the low dielectric constant and high rigidity of the crystal lattice, which inhibits the rotation to the most stable conformation of the TICT state. Although the TICT state may form in the crystal lattice, it would immediately convert back into the LE state. Furthermore, given the similarity of the spectrum in suspension to the T_1 observed in solution and the dissimilarity to the charge transfer states assigned by Mondal et al., we assign the long-lived transients to the T_1 state of benzophenones **2** and **3**. These assignments suggest that benzophenones **2** and **3** undergo intersystem crossing to the T_1 with rates of $2 \times 10^{11}\ s^{-1}$ and $4 \times 10^{10}\ s^{-1}$, respectively, and that they decay with time constants of 62 and 180 ps, respectively.

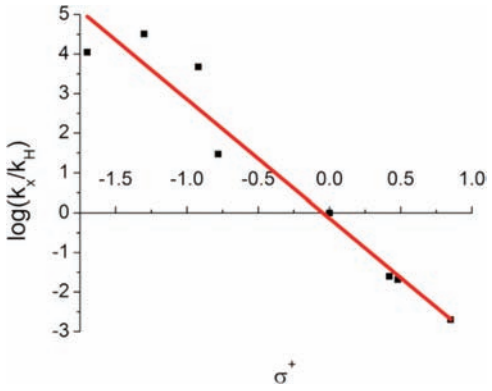

Figure 9. Hammett plot of the rate of quenching against the σ^+ Hammett constant, $\rho = -2.85$. In support of an n-type self-quenching mechanism in nanocrystalline suspensions of 4,4′-disubstituted benzophenones, the more electron-donating substituents quench the reaction faster.

Lifetime and Quenching of the Triplet States. The most striking difference between the solution and nanocrystalline suspension $T_1 \rightarrow T_n$ transient absorption spectra comes from their lifetimes. While T_1 lifetimes of the benzophenones with electron-rich substituents are significantly shorter in the nanocrystalline suspensions than in solution, the lifetimes of diacid **6**, diester **7**, and dianhydride **8** with electron-withdrawing substituents are either very similar or slightly longer (Table 1).

Having previously excluded the most obvious surface quenching mechanisms and multiphotonic interactions in the case of the parent ketone,[17] we turned our attention to self-quenching as a possible explanation for the reduced benzophenone lifetime. Self-quenching is defined as the quenching of an excited state molecule by interaction with another identical molecule that is in the ground state.[35] Self-quenching in benzophenone has been well-documented in solution with rates as high as 2.8×10^8 s^{-1}.[29] It should be noted that, in agreement with previous studies and in analogy with intramolecular quenching by β-aryl groups, we do not observe a formal charge-transfer species in our transient absorption measurements with nanocrystalline suspensions. This is consistent with the previously postulated "exciplex" mechanisms, leading to the ground state reactants without reaching a stable charge transfer state. The first of the two mechanisms, known as n-type quenching, involves electron donation from the ground state benzophenone aromatic ring into the electron-deficient oxygen lone pair orbital of the triplet n,π^* excited state. The second one, known as π-type quenching, involves the formal donation of an electron from the half-filled π^* orbital of the excited aromatic ketone into the empty π^* orbital of a neighboring ground state molecule.

The trend observed with compounds **1**−**8** clearly suggests a mechanism where electron donation occurs from the electron-rich aromatic rings to the electron-deficient carbonyl n-orbital. If we assume that all of the carbonyls have approximately the same electron affinity in the triplet excited state,[36] quenching will be primarily determined by the ground state electronics of the substituted benzophenones. As expected for an n-type mechanism, the relative rates of triplet decay in the nanocrystalline suspension plotted against the σ^+ Hammett values[37] of the corresponding substituents displayed an excellent correlation with $R^2 = 0.946$ and a slope of $\rho = -2.85$ (Figure 9). This is consistent with electron donation from the aromatic ring with development of a positive charge on the ground state donor. It is notable that the variation of decay rates spans 8 orders of magnitude, highlighting the significance of this effect, which could have important implications in the design of materials where triplet emission is desired, such as light-emitting diodes.

If one assumes that the observed decay rate (k_{dec}) in the nanocrystals is the sum of the intrinsic decay for an isolated molecule in dilute solution (k_i) plus the rate constant of self-quenching (k_{SQ}), one can estimate the latter in the solid state from the difference, $k_{SQ} = k_{dec} - k_i$. It should be noted that the approximate concentration of benzophenone in benzophenone crystals is on the order of 3−4 M, such that a qualitative comparison between the bimolecular rate constant of self-quenching in solution (M^{-1} s^{-1}) and the pseudounimolecular rate constant in the solid state (s^{-1}) may not be unreasonable (Table 2). As shown in Table 2, the reported self-quenching rate constants of benzophenone (**1**) and 4,4′-dimethoxybenzophenone (**5**) in benzene match very well with the values obtained in the solid state. However, the solution and solid state self-quenching rate constants in the case of 4,4′-bis(dimethylamino)benzophenone (**3**) differ by 2 orders of magnitude, with the solid state "catalyzing" this process. Another relatively large discrepancy can be seen when comparing the results for 4,4′-dimethylbenzophenone dicarboxylic acid, **6**. While self-quenching in solution is reported to occur very efficiently with a rate constant of 2.3×10^7 M^{-1} s^{-1}, deactivation in the solid state is 4 orders of magnitude less efficient with a value of 4.4×10^3 s^{-1}. In contrast to the linear Hammet plot shown in Figure 9, the results obtained in benzene solution by Wolf et al.[18] display two correlations with opposite slopes, with the lowest rate constant observed in the case of benzophenone. Noting that both electron- donating and electron-withdrawing substituents accelerate the rate constant of self-quenching of the substituted benzophenones, Wolf et al. suggested that self-quenching in solution occurs by two different pathways.

A plausible explanation for the different self-quenching behavior reported in solution and observed in the solid state may be based on the structural requirements for the self-quenching. Wolf et al.[18] proposed that the n-type and π-type mechanisms require different geometric arrangements between the aromatic ring and the carbonyl oxygen that are based on the requisite charge-transfer interactions. To define these geometries, we suggest a spherical coordinate system with the oxygen atom of the excited benzophenone as the origin, the plane of the carbonyl as a reference plane, and the C═O bond vector as the reference direction within the plane (Figure 10).

The quenching geometry under the coordinate system shown in Figure 10 can be defined in terms of a vector from the carbonyl oxygen to the interacting molecular orbital(s) in the aromatic ring. While the detailed geometry of this interaction is not known, for the sake of simplicity we will consider the aromatic ring centroid. One may expect that the plane of the interacting aromatic ring might be orthogonal to the connecting vector, **R**, so that the face of the ring is directly exposed to the excited carbonyl. For an n-type quenching, it is expected that the aromatic ring should be at a position given by an azimuth $\Theta = 60°$ to $\Theta = 90°$ in order to interact with the singly occupied n-orbital in the plane, an altitude $\Phi = 0°$ so that the centroid of the aromatic ring is bisected by the plane, and the shortest distance R given by van der Waals contact between the donor and the acceptor. By comparison, the optimal quenching geometry for π-type quenching might be expected when one of the aromatic rings approaches the carbonyl parallel to the plane of

Table 2. Comparison of Self-Quenching Rate Constants (k_{SQ}) in the Solid State and in Solution

benzophenone	k_i (s^{-1}), ACN[a]	k_{dec} (s^{-1}), solid[b]	k_{SQ} (s^{-1}), solid[c]	k_{SQ} (M^{-1} s^{-1}), C_6H_6
1 (H)	7.1×10^4	5.0×10^5	4.3×10^5	4.7×10^5
3 (NMe_2)	8.7×10^4	5.6×10^{10}	5.6×10^{10}	2.8×10^8
5 (OMe)	3.3×10^5	1.4×10^7	1.4×10^7	2.2×10^7
6 (COOMe)	5.8×10^3	1.0×10^4	4.4×10^3	2.3×10^7

[a] Decay rate constant in acetonitrile solution. [b] Decay rate constant in nanocrystalline suspension. [c] Estimated rate constant of self-quenching in the solid state.

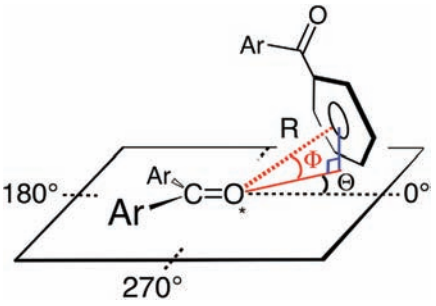

Figure 10. Definition of the spherical coordinates to describe the geometric parameters involved in quenching of the triplet benzophenone: **R** is the distance vector from oxygen atom to the centroid of the aromatic ring. The projection of **R** onto the plane is used to define the azimuth (Θ) and altitude (Φ) angles. The azimuth, Θ, is the angle formed between the projection of **R** and the reference direction, which is defined by a line along the C=O bond vector. The altitude, Φ, is measured from the projection of **R** on the plane to the **R** vector. Optimal n-type quenching is predicted to occur at $\Theta = 60-90°$ and $\Phi = 0°$.

the C=O bond to facilitate π-donor to π^*-acceptor interactions. The altitude should be $\Phi = 90°$ for the aromatic ring acceptor to be exactly above the carbonyl. Given this simple analysis, it was of interest to see whether such a geometric relationship holds in the crystalline solid state upon analysis of the corresponding single crystal X-ray structures.[38]

For each of the available X-ray structures with reported crystallographic information (cif) files, which includes benzophenones **1** (H), **2** (NH_2), **4** (OH), **5** (OMe), and **6** (COOH), we analyzed the position of the centroid of the aryl rings from all nearest neighbors of a given substituted benzophenone molecule in the crystal. These were found to be between 4 and 5 Å with azimuth angles between $\Theta = 90°$ and 120° and altitudes that ranged between $\Phi = 55°$ and 80°. Figure 11 shows a three-dimensional plot of the polar coordinates with the distance (R) and the azimuth angle (Θ) indicated in the plane and the value of the altitude (Φ) given by a color code. For all of the benzophenones, the nearest neighbor is in approximately the same region of space relative to the carbonyl oxygen. In every case, the closest aromatic groups have a position in space that is different from the values suggested by Wolf et al.[18] for either π quenching or n-type quenching. We found no obvious correlation between quenching rate constants and near neighbor structures.

Phenomenologically, the n-type self-quenching of benzophenone is similar to intramolecular β-aryl quenching of β-aryl acetophenones, which has been studied extensively in solution.[39] It has been suggested that β-aryl quenching occurs via a charge

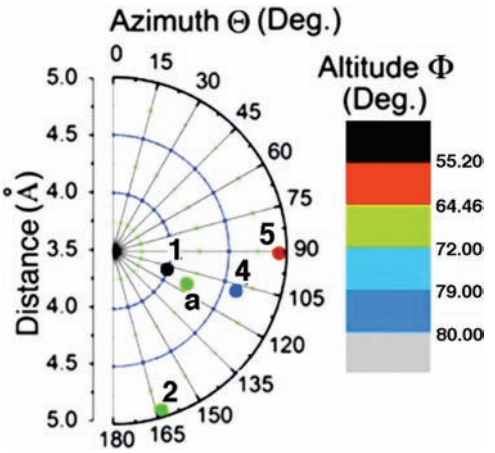

Figure 11. Three-dimensional polar contour plot showing the relative location (●) of the centroid of the nearest aryl quencher in space setting the carbonyl oxygen as the origin. The quenchers occupy a relatively small area of space. The data corresponds to benzophenones **1** (H), **2** (NH_2), **4** (OH), and **5** (OMe)[38] and the β-aryl quencher from ref 40b (a).

transfer mechanism where the β-aryl group formally donates an electron to the electron-deficient carbonyl during the quenching event. Analysis of the location of the quenching aryl ring with respect to the carbonyl oxygen in compounds that undergo β-aryl quenching in the solid state also appear in the same region of space as the ring of the nearest benzophenone neighbor (Figure 11, Θ=105°, R = 4.5 Å). For β-aryl quenching, it is proposed that the n-orbital of the carbonyl oxygen must point at the aryl moiety in a face-on relationship. In solution, the rate-determining step for β-aryl quenching is the attainment of this critical geometry.[19] From an examination of the known β-aryl quenchers in crystalline solids,[40] it appears that the geometry required for quenching in the solid state is relatively loose. Of the previously reported β-aryl quenchers, the aromatic groups deviate from a face-on relationship by 30−65° from the normal. Although not conforming to the assumed optimum geometry, their excited states are effectively quenched. Analyzing the crystal structures of the benzophenones in this study for deviations of the plane of the aromatic group from the normal to the vector drawn to the oxygen of the carbonyl, we found that all the aryl groups deviate from the face-on relationship by 24−44°. As before, no correlation was found between the rate constant of quenching and the amount of deviation from the normal. It should be pointed that recent calculations by Bucher et al. suggest an alternative mechanism for β-aryl quenching that involves the formation of a σ bond between the excited carbonyl oxygen and the *ipso*-carbon of the β-aryl group to form a short-lived ground state biradical species.[41] While a bond-forming mechanism could also operate in the intermolecular quenching case, the solid state geometries observed in the ketones studied here appear to be unfavorable for such a mechanism to operate.

Although it is thought that quenching primarily occurs via the n,π^* triplet states, Netto-Ferreira et al. have shown that the pre-exponential factor, A, for a series of phenylpropiophenones is insensitive to the nature of the low-lying triplet state.[39a] By this assumption, whenever the π,π^* state is lower in energy, thermal population of the T_2 (n,π)* must occur for effective quenching. For many of the benzophenones studied here, the difference in energy between T_2 and T_1 is relatively small, <3 kcal/mol,[36]

suggesting that population of the n,π^* excited state should be possible at ambient temperature within the lifetime of the excited state. However, for the 4,4′-bis(dimethylamino)benzophenone, **3**, with a triplet lifetime τ_T = 305 ps in suspension, the π,π^* triplet is lower by 20 kcal/mol, which makes it unlikely for thermal population of the n,π^* state to occur within such a short time scale. While one may suggest the involvement of a configurationally mixed excited state to engage a high-energy n,π^* triplet state, one may also consider an alternative reductive quenching mechanism from the π,π^* electronic configuration. In this case, formal electron transfer would occur from the ground-state aromatic ring of one molecule to the electron-deficient π-orbital of the π,π^* excited state. It may be expected that such an interaction would have a $\pi-\pi$ stacking geometry analogous to that postulated for the oxidative π-type quenching mechanism. While further analysis will be needed, the occurrence of reductive quenching from both excited state configurations and both interaction geometries are consistent with the results described.

■ CONCLUSIONS

We have reported the triplet lifetime and spectra for a series of 4,4′-disubstitued benzophenones in solution and as nanocrystalline suspensions obtained by a combination of femtosecond and nanosecond transient absorption spectroscopy and phosphorescence measurements. We report a remarkable self-quenching process for crystalline benzophenone triplet excited states with rate constants as high as 1.5×10^{10} s^{-1}. We have shown that the triplet excited states of nanocrystalline benzophenones **1**−**8** are deactivated by an intermolecular self-quenching mechanism consistent with reduction of the excited carbonyl. This is revealed by an excellent correlation between the self-quenching rate constants, which vary over 12 orders of magnitude, and the electron-donating abilities of the substituents in the aromatic groups. Furthermore, inspection of the crystal lattice of five of the eight benzophenones studied revealed a structural arrangement with the aromatic rings of their close neighbors occupying a similar region of space with geometries that suggest a relatively loose structural requirement for charge transfer quenching. This observation and the fact that reductive self-quenching occurs with ketones known to have either n,π^* and π,π^* configuration leads us to suggest the involvement of two reductive quenching mechanisms where formal charge transfer interactions involve the singly occupied n-orbital of ketones with an n,π^* configuration (n-type mechanism), or the lower lying singly occupied π^*-orbital of triplet ketones with a π,π^* excited state. We believe that this study highlights the potential of nanocrystalline suspensions as a medium to analyze excited states and transient kinetics within crystalline materials by time-resolved transmission spectroscopy methods.

■ EXPERIMENTAL SECTION

General Methods. The excitation and emission spectra of all samples were obtained on a Photon Technology International Quanta Master spectrofluorimeter. Dynamic light scattering measurements were taken on a Beckman-Coulter N4 Plus submicrometer particle size analyzer. Silica used for purification was Silica-P Flash silica gel (40−62 Å), purchased from SiliCycle Inc. UV−vis spectra were taken on a Beckman DU-650 spectrometer.

Nanocrystalline Suspensions. Nanocrystalline suspensions were synthesized via the reprecipitation method, which produces stable suspensions that can be easily transported in fluids such as water.[10] The crystalline nanoparticles were prepared by injecting a 0.4 M acetonitrile or tetrahydrofuran solution of the desired benzophenone into ca. 1000 times the volume of purified vortexing Millipore water (i.e., 4−10 μL of substrate into 4 mL water). In the case of the diacid **6**, a DMSO solution was used for the injection due to the low solubility of **6** in the other solvents. The resulting suspension (ca. 7×10^{-4} M) was sonicated three times at room temperature for 4 min, allowing for 2 min rest between runs. Suspensions produced in this manner were optically dense in a 1 cm cuvette at wavelengths below 355 nm, and their optical densities were adjusted by dilution to the values desired at the excitation wavelength (e.g., A = 0.05−0.10).

Nanosecond Transient Absorption Spectroscopy. Transient absorption experiments, based on nanosecond laser photolysis, were performed with the output of the third harmonics (355 nm) coming from a Nd/YAG laser (Brilliant, Quantel). Moreover, pulse widths of <5 ns with an energy of 10 mJ were selected. The optical detection is based on a pulsed Xenon lamp (XBO 450, Osram), a monochromator (Spectra Pro 2300i, Acton Research), a R928 photomultiplier tube (Hamamatsu Photonics), or a fast InGaAs photodiode (Nano 5, Coherent) with amplification of 500 MHz and a digital oscilloscope (1 GHz; WavePro7100, LeCroy). The laser power of every laser pulse was registered by using a bypath with a fast silicon photodiode. The nanosecond laser photolysis experiments were performed with 1-cm quartz cells and the solutions, at concentrations that were low enough to avoid the self-quenching observed in solution, were saturated with argon if no other gas saturation is indicated and stirred vigorously during the experiment. The lifetimes were acquired in a minimum of triplicate. We confirmed that there was no sample degradation after data acquisition.

Femtosecond Transient Absorption Spectroscopy. Femtosecond transient absorption studies were performed with 258 nm laser pulses (1 kHz, 150 fs pulse width) from an amplified Ti/sapphire laser system (model CPA 2101, Clark-MXR Inc.; output 775 nm). The transient absorption pump−probe spectrometer (TAPPS) was referred to as a two-beam setup, where the pump pulse was used as excitation source for transient species and the delay of the probe pulse was exactly controlled by an optical delay rail. As probe (white light continuum), a small fraction of pulses stemming from the CPA laser system was focused by a 50 mm lens into a 2-mm thick sapphire disk. The transient spectra were recorded using fresh, oxygen-free solutions or freshly prepared nanocrystalline suspensions. All experiments were performed at 298 K in a 2 mm quartz cuvette. We confirmed that there was no sample degradation after data acquisition.

Quenching Experiments. Nanosecond laser flash photolysis at 355 nm of benzophenone suspensions (3 mL) was conducted in argon-saturated suspensions. To minimize changes in ground-state absorption, a small volume (1 μL) of the inorganic salt (KI, NaI, NaBr, NaN_3) in Millipore water (typically 0.1−1 M) was added to the suspension, which was then mixed thoroughly. The $T_1 \rightarrow T_n$ Stern−Volmer quenching data was recorded at 515 nm for an average of 120 laser shots for all suspensions. The resulting Stern −Volmer quenching plots were acquired in at least triplicate.

Phosphoresence Lifetime Measurements. The third harmonic (355 nm) output of a Quantel Brilliant Nd/YAG laser was used for triplet-state lifetime measurements (<5 ns pulse width, ∼60 mJ/pulse). Time-resolved and steady-state luminescence spectra were obtained with a 0.3 m monochromator coupled to a Roper Scientific PIMAX gated, intensified CCD (emission was collected at a right angle with respect to the laser irradiation).

Dynamic Light Scattering (DLS). The DLS measurements were conducted using a Beckman-Coulter N4 Plus particle analyzer with a 10 mW helium−neon laser at 632.8 nm. The particle size was determined using a detector angle of 90°, and it was calculated using the size distribution processor (SDP) analysis package provided by the manufacturer. A reasonable match was obtained by scanning electron microscopy (SEM).

Scanning Electron Microscopy (SEM). Benzophenone nanocrystals obtained by the reprecipitation protocol were analyzed by SEM to verify the size, shape, and formation of crystal faces. SEM studies were performed with a JEOL JSM-6700F field-emission scanning electron microscope. To prepare the SEM sample, a dilute benzophenone suspension (4×10^{-4} M) was drop-cast onto a freshly cleaned silicon wafer and allowed to dry in a desiccator. Both isolated crystals and aggregates consisting of 2−10 crystals were observed. Figure 1 shows benzophenone nanocrystals with sizes ranging between ca. 200 and 500 nm, in general agreement with the DLS results from the fluid suspension. The particles are clearly faceted and crystalline.

■ ASSOCIATED CONTENT

Supporting Information. UV−vis spectra, dynamic light scattering (DLS), differential scanning calorimetry, transient absorption spectra, transient decays, and SEM images. This material is available free of charge via the Internet at http://pubs.acs.org.

■ AUTHOR INFORMATION

Corresponding Author
mgg@chem.ucla.edu

■ ACKNOWLEDGMENT

We are grateful to the National Science Foundation for support through Grants CHE-0844455, DMR0605688, creativity extension DMR0937243, and DGE0114443 (IGERT MCTP) for a training fellowship to G.K., and to Deutsche Forschungsgemeinschaft - SFB 583 - for funding. We dedicate this manuscript to Professor Tomas Torres on the occasion of his 60th birthday.

■ REFERENCES

(1) (a) Spano, F. C. *Annu. Rev. Phys. Chem.* **2006**, *57*, 217. (b) Spano, F. C. *Acc. Chem. Res.* **2010**, *43*, 429. (c) Shimizu, M.; Hiyama, T. *Chem.—Asian J.* **2010**, *5*, 1516. (c) Lim, S. H.; Bjorklund, T. G.; Spano, F. C.; Bardeen, C. *J. Phys. Rev. Lett.* **2004**, *92*, No. 107402. (d) Andrew, T. L.; Swager, T. M. *J. Polym. Sci., Part B* **2011**, *49*, 476. (e) Davis, R.; Kumar, N. S. S.; Abraham, S.; Suresh, C, H.; Rath, N. P.; Tamaoki, N.; Das, S. *J. Phys. Chem. C* **2008**, *112*, 2137. (f) Anthony, J. E.; Brooks, J. S.; Eaton, D. L.; Parkin, S. R. *J. Am. Chem. Soc.* **2003**, *123*, 9482. (g) Duxbury, D. F. *Chem. Rev.* **1993**, *93*, 381. (h) Kobatake, S.; Takami, S.; Muto, H.; Ishikawa, T.; Song, A. K. S. *Curr. Opin. Solid State Mater. Sci.* 1996, *1*, 834. (i) Irie, M. *Nature* **2007**, *446*, 778. (j) Ikeda, T.; Tsutsumi, O. *Science* **1995**, *268*, 5219.

(2) (a) Morimoto, M.; Irie, M. *J. Am. Chem. Soc.* **2010**, *132*, 14172. (b) Garcia-Garibay, M. A. *Angew Chem., Int. Ed.* **2007**, *46*, 8945. (c) Lebedeva, N. V.; Tarasov, V. F.; Resendiz, M. J. E.; Garcia-Garibay, M. A.; White, R. C.; Forbes, M. D. E. *J. Am. Chem. Soc.* **2010**, *132*, 82. (d) Macgillivray, L. R.; Papaefstathiou, G. S.; Friscic, T.; Hamilton, T. D.; Bucar, D. K.; Chu, Q.; Varshney, D. B.; Georgiev, I. G. *Acc. Chem. Res.* **2008**, *41*, 280. (e) Hollingsworth, M. D.; McBride, J. M. *Adv. Photochem.* **1990**, *15*, 279–379. (f) Garcia-Garibay, M. A. *Acc. Chem. Res.* **2003**, *36*, 491. (g) Zimmerman, H. E.; Nesterov, E. E. *Acc. Chem. Res.* **2002**, *35*, 77. (h) Desiraju, G. R. *Organic Solid State Chemistry*; Elsevier: Amsterdam, 1987. (i) Ramamurthy, V.; Venkatesan, K. *Chem. Rev.* **1987**, *87*, 433–481.

(3) (a) Michl, J. *Chem. Rev.* **2010**, *110*, 6891. (b) Thorsmølle, V. K.; Averitt, R. D.; Demsar, J.; Smith, D. L.; Tretiak, S.; Martin, R. L.; Chi, X.; Crone, B. K.; Ramirez, A. P.; Taylor, A. J. *Phys. Rev. Lett.* **2009**, *102*, No. 017401. (c) Takeda, Y.; Katoh, R.; Kobayashi, H.; Kotani, M. *J. Electron Spectrosc. Relat. Phenom.* **1996**, *78*, 423. (d) Ruiz Delgado, M. C.; Kim, E.-G.; da Silva Filho, D. A.; Bredas, J.-L. *J. Am. Chem. Soc.* **2010**, *132*, 3375.

(4) (a) van Dijken, A.; Brunner, K.; Boerner, H.; Langeveld, B. M. W. *Highly Efficient OLEDs with Phosphorescent Materials*; Yersin, H., Ed.; Wiley-VCH: Berlin, 2008; p 311. (b) Sun, Y.; Forrest, S. R. *Nat. Photonics* **2008**, *2*, 483. (c) Shen, Z.; Burrows, P. E.; Bulovic, V.; Forrest, S. R.; Thompson, M. E. *Science* **1997**, *276*, 2009. (d) Sun, Y.; Giebink, N. C.; Kanno, H.; Ma, B.; Thompson, M. E.; Forrest, S. R. *Nature* **2006**, *440*, 908. (e) Bolton, O.; Lee, K.; Kim, H.-J.; Lin, K. Y.; Kim, J. *Nat. Chem.* **2011**, *3*, 207.

(5) (a) Peet, J.; Kim, J. Y.; Coates, N. E.; Ma, W. L.; Moses, D.; Heeger, A. J.; Bazan, G. C. *Nat. Mater.* **2007**, *6*, 497. (b) Varotto, A.; Treat, N. D.; Jo, J.; Shuttle, C. G.; Batara, N. A.; Brunetti, F. G.; Seo, J. H.; Chabinyc, M. L.; Hawker, C. J.; Heeger, A. J.; Wudl, F. *Angew. Chem.* **2011**, *50*, 5166. (c) Mauldin, C. E.; Piliego, C.; Poulsen, D.; Unruh, D. A.; Woo, C.; Ma, B.; Mynar, J. L.; Fréchet, J. M. J. *ACS Appl. Mater. Interfaces* **2010**, *2*, 2833.

(6) (a) Burns, G. *Solid State Physics*; Academic Press: San Diego, CA, 1985. (b) Nye, J. F. *Physical Properties of Crystals. Their Representation by Tensors and Matrices*; Oxford University Press: Oxford, U.K., 1985. (c) Kaminsky, W.; Clabrown, K.; Kahr, B. *Chem. Soc. Rev.* **2004**, *33*, 514.

(7) (a) Kuzmanich, G.; Gard, M. N.; Garcia-Garibay, M. A. *J. Am. Chem. Soc.* **2009**, *131*, 11606. (b) Kuzmanich, G.; Natarajan, A.; Chin, K. K.; Veerman, M.; Mortko, C. J.; Garcia-Garibay, M. A. *J. Am. Chem. Soc.* **2008**, *130*, 1140.

(8) Swenberg, C. E.; Gaecintov, N. E. In *Organic Molecular Photophysics*; Birks, J. B., Ed.; John Wiley & Sons: London, 1973; p 489.

(9) (a) Wilkinson, F.; Kelly, G. In *Handbook of Organic Photochemistry*; Scaiano, J. C., Ed.; CRC Press: Boca Raton, FL, 1989; Vol. 1, 293. (b) Kessler, R. W.; Krabichler, G.; Uhl, S.; Oelkrug, D.; Hagan, W. P.; Hyslop, J.; Wilkinson, F. *Opt. Acta* **1983**, *30*, 1099.

(10) Kasai, H.; Nalwa, H. S.; Oikawa, H.; Okada, S.; Matsuda, H.; Minami, N.; Kuakuta, A.; Ono, K.; Mukoh, A.; Nakanishi, H. *Jpn. J. Appl. Phys.* **1992**, *31*, 1132.

(11) (a) Gesquiere, A. J.; Uwada, T.; Asahi, T.; Masuhara, H.; Barbara, P. F. *Nano Lett.* **2005**, *5*, 1321. (b) Kim, H. Y.; Bjorklund, T. G.; Lim, S.-H.; Bardeen, C. J. *Langmuir* **2003**, *19*, 3941. (c) Matsune, H.; Asahi, T.; Masuhara, H.; Kasai, H.; Nakanishi, H. *Mater. Res. Soc. Symp. Proc.* **2005**, *846*, 263. (d) Möler, S.; Weiser, G.; Taliani, C. *Chem. Phys.* **2003**, *295*, 11. (e) Patra, A.; Hebalkar, N.; Sreedhar, B.; Sarkar, M.; Samanta, A.; Radhakrishnan, T. P. *Small* **2006**, *2*, 650.

(12) Kuzmanich, G.; Spänig, F.; Tsai, C.-K.; Um, J. M.; Hoekstra, R. M.; Houk, K. N.; Guldi, D. M.; Garcia-Garibay, M. A. *J. Am. Chem. Soc.* **2011**, *133*, 2342.

(13) Chin, K. K.; Natarajan, A.; Gard, M. N.; Campos, L. M.; Johansson, E.; Shepherd, H.; Garcia-Garibay, M. A. *Chem. Commun.* **2007**, *41*, 4266.

(14) Schuster, D. I.; Weil, T. M. *J. Am. Chem. Soc.* **1973**, *95*, 4091.

(15) Parker, C. A.; Joyce, T. A. *Chem. Commun.* **1968**, 749.

(16) Wilkinson, F.; Willsher, C. J. *Chem. Phys. Lett.* **1984**, *104*, 272.

(17) Simoncelli, S.; Kuzmanich, G.; Gard, M. N.; Garcia-Garibay, M. A. *J. Phys. Org. Chem.* **2010**, *23*, 376.

(18) Wolf, M. W.; Legg, K. D.; Brown, R. E.; Singer, L. A.; Parks, J. H. *J. Am. Chem. Soc.* **1975**, *97*, 4490.

(19) Schuster, D. I.; Weil, T. M.; Halpern, A. M. *J. Am. Chem. Soc.* **1972**, *94*, 8284.

(20) Guttenplan, J. B.; Cohen, S. G. *J. Am. Chem. Soc.* **1972**, *94*, 4040.

(21) Favaro, G. *Chem. Phys. Lett.* **1973**, *21*, 401.

(22) Favaro, G. *J. Photochem.* **1986**, *35*, 375.

(23) The average standard deviation was approximately one-half of the mean particle size.

(24) (a) Palit, D. K. *Res. Chem. Intermed.* **2005**, *31*, 205. (b) Tosh, S. B.; Chattopadhyay, S. K.; Das, P. K. *J. Phys. Chem.* **1984**, *88*, 1404.

(25) Wang, G.-C.; Winnik, M. A. *J. Photochem.* **1986**, *33*, 291.

(26) Singh, A. K.; Bhasikuttan, A. C.; Palit, D. K.; Mittal, J. P. *J. Phys. Chem. A* **2000**, *104*, 7002.

(27) Bhasikuttan, A. C.; Singh, A. K.; Palit, D. K.; Sapre, A. V.; Mittal, J. P. *J. Phys. Chem. A* **1998**, *102*, 3470.

(28) DMSO was chosen for 4,4′-dicarboxybenzophenone because ODs of 0.3 were unobtainable in other solvents due to sample insolubility.

(29) Shizuka, H.; Obuchi, H. *J. Phys. Chem.* **1982**, *86*, 1297.

(30) Ferguson, G.; Glidewell, C. *Acta Crystallogr., Sect. C. Cryst. Struct. Commun.* **1996**, *52*, 3057.
(31) Ohtani, H.; Kobayashi, T.; Suzuki, K.; Nagakura, S. *Bull. Chem. Soc. Jpn.* **1980**, *53*, 43.
(32) Mondal, J. A.; Ghosh, H. N.; Ghant, T. K.; Mukherjee, T.; Palit, D. K. *J. Phys. Chem. A* **2006**, *110*, 3432.
(33) Singh, A. K.; Palit, D. K.; Mittal, J. P. *Res. Chem. Intermed.* **2001**, *27*, 125.
(34) Pal, T.; Paul, M.; Ghosh, S. *J. Mol. Struct.: THEOCHEM* **2008**, *860*, 8.
(35) Verhoeven, J. W. *Pure Appl. Chem.* **1996**, *68*, 2223.
(36) Murov, S. L.; Carmichael, I.; Hug, G. L. *Handbook of Photochemistry*, 2 ed.; Marcel Dekker, Inc.: New York, 1993.
(37) Corwin, H.; Leo, A.; Taft, R. W. *Chem. Rev.* **1991**, *91*, 156. σ^+ Hammett values: H, 0; NH_2, −1.3; NMe_2, −1.7; OH, −0.92; OMe, −0.78; COOH, 0.42; COOMe, 0.18; **8**, 0.85 (Summation of σ^+ COOR + σ_m COOR).
(38) **1**:Fleischer, E. B.; Sung, N.; Hawkinson, S. *J. Phys. Chem.* **1968**, *72*, 4311. Space Group: $P2_12_12_1$ (a = 10.300, b = 12.150, c = 8.000, $\alpha = \beta = \gamma = 90°$). **2**:Genbo, S.; Shouwu, G.; Feng, P.; Youping, H.; Zhengdong, L. *J. Phys. D: Appl. Phys.* **1993**, *26*, B236. Space Group: $P3_1$ ($a = b$ = 9.136, c = 10.953, $\alpha = \beta = 90°$, $\gamma = 120°$). **4**:Ferguson, G.; Gildewell, C. *Acta Crystallogr., Sect. C: Cryst. Struct. Commun.* **1996**, *52*, 3057. Space Group: $P2_1/c$ (a = 9.450, b = 24.456, c = 9.484, $\alpha = \gamma = 90°$, β = 103.61°). **5**:Norment, H. G.; Karle, I. L. *Acta Crystallogr.* **1962**, *15*, 873Space Group: $P2_1/a$ (a = 16.430, b = 16.030, c = 9.620, $\alpha = \gamma = 90°$, β = 100.85°).
(39) (a) Netto-Ferreira, J. C.; Leigh, W. J.; Scaiano, J. C. *J. Am. Chem. Soc.* **1985**, *107*, 2617. (b) Scaiano, J. C.; Perkins, M. J.; Sheppard, J. W.; Platz, M. S.; Barcus, R. L. *J. Photochem.* **1983**, *21*, 137. (c) Leigh, W. J.; Banisch, J.-A. H.; Workentin, M. S. *J. Chem. Soc., Chem. Commun.* **1993**, 988.
(40) (a) Boch, R.; Bohne, C.; Scaiano, J. C. *J. Org. Chem.* **1996**, *61*, 1423. (b) Ng, D.; Yang, Z.; Garcia-Garibay, M. A. *Tetrahedron Lett.* **2001**, *42*, 9113.
(41) (a) Smith, M. J.; Bücher, G. *J. Phys. Chem. A* **2010**, *114*, 10712. (b) Bücher, G. *J. Phys. Chem. A* **2008**, *112*, 5411.